0021-972X/07/$15.00/0
Printed in U.S.A.

The Journal of Clinical Endocrinology & Metabolism 92(4):1237–1244

doi: 10.1210/jc.2006-1479

Fluorine-18-L-Dihydroxyphenylalanine (^{18}F-DOPA) Positron Emission Tomography as a Tool to Localize an Insulinoma or β-Cell Hyperplasia in Adult Patients

Saila Kauhanen, Marko Seppänen, Heikki Minn, Risto Gullichsen, Anna Salonen, Kalle Alanen, Riitta Parkkola, Olof Solin, Jörgen Bergman, Timo Sane, Jorma Salmi, Matti Välimäki, and Pirjo Nuutila

Turku PET Centre (S.K., M.S., A.S., R.P., P.N.), and Departments of Surgery (S.K., R.G.), Oncology and Radiotherapy (H.M.), and Pathology (K.A.), Turku University Hospital, FIN-20520 Turku, Finland; Turku PET Centre (O.S., J.B.), Radiopharmaceutical Chemistry Laboratory, University of Turku, FIN-20520 Turku, Finland; Department of Medicine (T.S., M.V.), Helsinki University Hospital, FIN-00029 Helsinki, Finland; and Department of Medicine (J.S.), Tampere University Hospital, FIN-33014 Tampere, Finland

Context and Objective: Fluorine-18-L-dihydroxyphenylalanine (^{18}F-DOPA) positron emission tomography (PET) is a promising method in localizing neuroendocrine tumors. Recently, it has been shown to differentiate focal forms of congenital hyperinsulinism of infancy. The current study was set up to determine the potential of ^{18}F-DOPA PET in identifying the insulin-secreting tumors or β-cell hyperplasia of the pancreas in adults.

Patients and Methods: We prospectively studied 10 patients with confirmed hyperinsulinemic hypoglycemia and presumed insulin-secreting tumor using ^{18}F-DOPA PET. Anatomical imaging was performed with computed tomography (CT) and magnetic resonance imaging (MRI). All patients were operated on, and histological verification was available in each case. Semiquantitative PET findings in the pancreas using standardized uptake values were compared to standardized uptake values of seven consecutive patients with nonpancreatic neuroendocrine tumors.

Results: By visual inspection of ^{18}F-DOPA PET images, it was possible in nine of 10 patients to localize the pancreatic lesion, subsequently confirmed by histological analysis. ^{18}F-DOPA uptake was enhanced in six of seven solid insulinomas and in the malignant insulinoma and its hepatic metastasis. Two patients with β-cell hyperplasia showed increased focal uptake of ^{18}F-DOPA in the affected areas. As compared to CT or MRI, ^{18}F-DOPA PET was more sensitive in localizing diseased pancreatic tissue.

Conclusion: ^{18}F-DOPA PET was useful in most patients with insulinoma and negative CT, MRI, and ultrasound results. In agreement with previous findings in infants, preoperative ^{18}F-DOPA imaging seems to be a method of choice for the detection of β-cell hyperplasia in adults. It should be considered for the detection of insulinoma or β-cell hyperplasia in patients with confirmed hyperinsulinemic hypoglycemias when other diagnostic work-up is negative. **(*J Clin Endocrinol Metab* 92: 1237–1244, 2007)**

IN ADULTS, INSULINOMA is the most common cause of hyperinsulinemic hypoglycemia (1–4). Most often (90%) these neoplasms turn out to be benign single focal lesions in the pancreas, but 10% present as malignant and in multiple forms. In very rare cases, insulinoma can also show an ectopic localization (5, 6). The early diagnosis is mainly based on symptoms and biochemical proof of hyperinsulinemic hypoglycemia (6). Persistent hyperinsulinemic hypoglycemia (PHH) in adults can also be caused by pancreatic β-cell hyperplasia (nesidioblastosis). This entity was first described in infants (7), but since 1971 there have been more and more reports of β-cell hyperplasia associated with hyperinsulinemic hypoglycemia among adults as well (1, 2, 8–10). Recent retrospective reports have indicated that approximately 4–5% of adult patients with PHH are affected by β-cell hyperplasia (2, 10).

After diagnosis of organic hyperinsulinism, surgical enucleation of the tumor or partial pancreatic resection is the primary mode of treatment. The conventional imaging studies [ultrasound, computed tomography (CT), magnetic resonance imaging (MRI), angiography, intraarterial calcium stimulation with venous sampling, endoscopic ultrasound (EUS), and somatostatin receptor scintigraphy (SRS)] have been the cornerstone for tumor localization in patients with insulinoma or β-cell hyperplasia. However, so far, all these methods either have limited sensitivity or are invasive procedures (11).

Positron emission tomography (PET) combined with fluorine-18-L-dihydroxyphenylalanine (^{18}F-DOPA) has been used for more than two decades to investigate the activity of the dopaminergic system *in vivo* in neurological disorders. Neuroendocrine tumors (NETs) have the capacity to take up and decarboxylate amine precursors like L-DOPA and 5-hydroxy-L-tryptophan (12). Furthermore, the endocrine pancreas has been shown to have an efficient mechanism for the uptake and decarboxylation of L-DOPA, converting it to dopamine (13, 14). There has also been some promising ex-

First Published Online January 16, 2007

Abbreviations: CI, Confidence interval; CT, computed tomography; CV, coefficient of variation; EUS, endoscopic ultrasound; ^{18}F-DOPA, fluorine-18-L-dihydroxyphenylalanine; MRI, magnetic resonance imaging; NET, neuroendocrine tumor; PHH, persistent hyperinsulinemic hypoglycemia; PET, positron emission tomography; SRS, somatostatin receptor scintigraphy; SUV, standardized uptake values.

JCEM is published monthly by The Endocrine Society (http://www.endo-society.org), the foremost professional society serving the endocrine community.

perience of diagnosing pancreatic NETs using tracers like ^{11}C-5-hydroxy-L-tryptophan and ^{64}Cu-TETA-octreotide, in addition to ^{11}C-DOPA (15–17). ^{18}F-DOPA PET has been successfully used in the imaging of carcinoid tumors, glomus tumors, pheochromocytomas, and medullary thyroid cancers (18–21). In 2004 Becherer *et al.* (22) studied 23 patients with advanced NETs using ^{18}F-DOPA, including three successful diagnoses of pancreatic NET, and found ^{18}F-DOPA to be useful in the staging of diseases.

Recently, we and others have demonstrated the usefulness of ^{18}F-DOPA PET in the detection of focal β-cell hyperplasia (23, 24) and ectopic lesion (25) in congenital hyperinsulinism of infancy. Concurrently, with infant studies, we have conducted another prospective research protocol to determine the potential of ^{18}F-DOPA PET to identify and precisely localize the insulin-secreting tumors of the pancreas in adults. Our aim has been to compare PET findings with the established imaging methods. This report summarizes our current results from eight consecutive adult patients with insulinoma and two patients with β-cell hyperplasia. We compare the diagnostic sensitivity of ^{18}F-DOPA PET with conventional methods in hyperinsulinemic and hypoglycemic adults. Furthermore, the outcome of these 10 patients is described.

Patients and Methods

Study patients

Ten consecutive patients (five females, five males; mean age, 49 ± 13 yr) with confirmed hyperinsulinemic hypoglycemic episodes were referred to the PET Centre in Turku, Finland, between April 2001 and January 2006 (Table 1). All patients had symptoms of neuroglycopenia associated with inappropriately elevated levels of insulin in relation to decreased glucose levels. The study patients fulfilled the diagnostic biochemical criteria of hyperinsulinemic hypoglycemia, with a mean glucose value of 2.2 mmol/liter, a concomitant mean insulin level of 41 mU/liter, and a mean C-peptide level 1.69 nmol/liter. The mean duration of symptoms before diagnosis was more than 3 yr, and mean body mass index was 29.1 ± 5.4 kg/m^2 (Table 1). More details about patient histories are given in *Results*. All patients were studied with ^{18}F-DOPA PET. PET results were compared with the pancreatic ^{18}F-DOPA uptake of seven consecutive patients (three females, four males; mean age, 47 ± 16 yr; body mass index, 24.6 ± 1.9 kg/m^2) with suspected extraadrenal or adrenal neuroendocrinological disease. None of these had any suspicion of pancreatic disease. Two of seven control patients had cortical adrenal adenoma, one patient had a malignant pheochromocytoma, one patient had a suspicion of recurrent adrenal pheochromocytoma, and three patients had no NETs.

Preoperative studies also included CT and MRI. In addition, intraoperative ultrasound (patient 1), EUS (patients 7, 8, and 10), and SRS (patients 1 and 8) were performed. All patients with hyperinsulinism were operated on, and the histological confirmation of the disease was received. The study was conducted according to the guidelines of the Declaration of Helsinki, and the study protocol was approved by the ethics committee of the Hospital District of Southwest Finland and the Finnish National Agency for Medicine. All patients gave their written informed consent before participating in the study.

^{18}F-DOPA PET

Patients fasted for at least 6 h before the PET scan. If the patient was using medication that prevents pancreatic insulin release (diazoxide, somatostatin analogs, or cortisone), the medication was withdrawn 24 h before the study. Plasma glucose level was monitored, and a glucose (G5%–G10%, 40–100 ml/h) infusion was given, if needed, to keep plasma glucose between 4.0 and 5.0 mmol/liter.

^{18}F-DOPA was synthesized according to previously described methods (26). The average iv injected dose of ^{18}F-DOPA was 234 ± 71 MBq (range, 160–362). Scanning began 60 min after injection. Patients underwent a whole-body PET scan from the level of the eyes to the thigh with a GE Advanced PET scanner (General Electric Medical Systems,

TABLE 1. Characteristics of the study patients

Patient no.	Gender	Age at PET (yr)	Duration of symptoms (yr)	Standard fasting test			PET[a]	Surgery (palpation focus in operation)	Histology	Outcome
				Blood glucose (mmol/liter)	Insulin (mU/liter)	c-Peptide (nmol/liter)				
1	F	34	2	1.9	220.0	4.4	Head	Subtotal pancreatectomy (−)	Nesidioblastosis	Cured
2	M	63	2	2.0	24.0	1.8	Head	Subtotal pancreatectomy and splenectomy (−)	Nesidioblastosis	Symptoms
3	M	58	4	2.1		1.3	Tail[b]	Resection of tail and splenectomy (body/tail)	Insulinoma	Cured
4	F	59	Several	3.0	10.0	0.76	Tail	Resection of tail (tail)	Insulinoma	Cured
5	F	55	3	2.6	10.0	1.8	Body[c]	Resection of body and tail (body)	Malignant insulinoma	Death[c]
6	F	61	10	1.8	39.0	2.4	Head	Enuceation (head)	Insulinoma	Death[d]
7	M	23	1	2.0	29.0	1.51	Indeterminate[e]	Resection of body and tail (body/tail)	Insulinoma	Cured
8	M	46	1	2.2	14.0	1.17	Head	Enucleation (head/body)	Insulinoma	Cured
9	M	53	2	2.2		0.87	Head	Pancreaticoduodenectomy (head)	Insulinoma	Cured
10	F	38	5	2.4	9.3	0.72	Body[b]	Enucleation (body)	Insulinoma	Cured

[a] The location of highest mean SUV value.
[b] The maximum SUV was classified as being intermediate between body and tail of pancreas.
[c] The maximun SUV was classified as being intermediate between head and body of pancreas. Liver metastasis was seen in PET, CT, and MRI, whereas the pancreatic primary tumor was not found by CT or MRI. The patient subsequently died due to disease's progression.
[d] No recovery postoperatively due to severe pancreatitis.
[e] Abundance of radioactivity in bile in common bile duct covering the head of pancreas disturbed evaluation the tracer uptake in different parts of the pancreas.

Milwaukee, WI) operated in two-dimensional mode. The scanner consists of 18 rings of bismuth germinate detectors yielding 35 transverse slices spaced at 4.25-mm intervals. The diameter of the imaging field of view is 55 cm, and the axial length is 15.2 cm.

To obtain images for visual and semiquantitative analysis, the data were corrected for dead time, decay, and photon attenuation, and reconstructed in a 128 × 128 matrix. The final in-plane resolution in segmented attenuation correction and iterative-reconstructed and Hann-filtered (4.6 mm) image was 5 mm (full-width half-maximum).

PET images were analyzed visually and semiquantitatively by calculating mean and maximum standardized uptake values (SUVs) in the region of interest drawn separately on the pancreatic head, body, and tail. Axial, coronal, and sagittal views were evaluated, and the pancreas invariably had a sufficiently high uptake of ^{18}F-DOPA to distinguish it from the liver, duodenum, and kidneys. Variable uptake was seen in the gallbladder and biliary duct. Pancreatic tissue uptake of PET images was always correlated side by side with anatomical reference images of CT or MRI. Interpretation was based on consensus of two specialists with significant experience in PET imaging (M.S. and H.M.), and there was no disagreement.

CT

All patients were examined with CT. Seven of 10 patients were imaged on a four-row CT scanner (Siemens Volume Zoom; Siemens, Erlangen, Germany), and three patients were imaged on a one-row CT scanner (Siemens Somatom Plus, Siemens). In all examinations, the reconstructed final transverse slice thickness was either 5 or 6 mm. Four patients (no. 1, 2, 3, and 5) were imaged without contrast injection and after contrast administration both in arterial and venous phase. Six patients were imaged without contrast and postcontrast venous phase.

MRI

MRI imaging was performed at 1.5 T (Vision or Symphony; Siemens Medical System, Erlangen, Germany) on six patients and at 1.5 T (Genesis Sigma; General Electric Medical Systems) on one patient. Five patients (no. 1, 2, 5, 9, and 10) were imaged on Symphony with the following pulse sequences: transverse T2-weighted images with and without fat saturation, and transverse T1-weighted images with slice thickness of 5 mm, in addition to axial T1-weighted images with and without administration of contrast agent, gadopentetate dimeglumine (Magnevist; Schering AG, Berlin, Germany). The T1-weighted sequence was performed after iv administration of Magnevist followed by a saline flush, *i.e.* in precontrast, arterial, venous, and steady-state phases. One patient (no. 7) was imaged with Vision with the following pulse sequences: transverse and coronal T2-weighted images with slice thickness of 5 mm, transverse T2-weighted images with slice thickness of 6 mm, and T1-weighted images with fat saturation with and without Magnevist. One patient (no. 8) was imaged with Genesis Sigma with the following pulse sequences: transverse T2-weigted images with and without fat saturation, transverse T1-weigted phase images, coronal T2-weighted images with fat saturation, and transverse T1-weighted gradient-refocused images with fat saturation. This last sequence was performed with and without administration of Magnevist in precontrast, arterial, venous, and steady-state phases.

Histological analysis

The primary diagnosis was performed using 4-μm-thick, van Gieson-stained sections cut from paraffin blocks. The immunohistochemical staining was performed using automated immunostainer (TechMate 500, DakoCytomation; Dako, Glostrup, Denmark). Sections were dried overnight at room temperature and kept at 60 C for 1 h. This was followed by antigen retrieval in ChemMate (DakoCytomation) solution in a microwave oven twice before immunohistochemical staining. Primary antibody incubation was followed by incubation with a ChemMate detection kit, based on the indirect streptavidin biotin method, with a biotinylated link antibody. Endogenous peroxidase treatment was followed by incubation with streptavidin conjugate labeled with horseradish peroxidase. Diaminobenzedine was used as a chromogen, followed by light Mayer's hematoxylin nuclear counterstaining.

Statistical analysis

Coefficient of variation (CV) was used to assess intrapatient variations. The Mann-Whitney *U* test was used to compare the variables (CV%) between groups. Sensitivity was calculated in each imaging method (PET, CT, and MRI). A McNemar test was performed to compare PET, CT, and MRI, and κ coefficient was determined to quantify agreement of these imaging methods. $P < 0.05$ was considered statistically significant. All statistical analyses were conducted using SPSS statistical software (version 13.0; SPSS Inc., Chicago, IL).

Results

Final diagnoses and representative cases

Histological confirmation of diagnosis was obtained in all of 10 study patients. Two patients had focal β-cell hyperplasia (patients 1 and 2), seven had solitary benign insulinoma, and one patient (no. 5) had malignant insulinoma.

Patients with β-cell hyperplasia. A 34-yr-old woman (patient 1) had been otherwise healthy except for a history of preeclampsias during pregnancies and low plasma glucose concentrations after delivery. In March 2001, during a varicose vein operation, the patient had a hypoglycemic episode with seizure and she was admitted to our hospital. She needed continuous glucose infusion to maintain euglycemia. During hypoglycemia, serum insulin level was 220 mU/liter and that of plasma C-peptide 4.4 nmol/liter (Table 1). CT, MRI, angiography, and SRS were all normal. At explorative laparotomy, the pancreas was regarded as normal including a negative intraoperative ultrasound finding. Before pancreatectomy, it was decided to try to localize the hyperfunctional focus using ^{18}F-DOPA PET. PET imaging showed enhanced tracer uptake in the head of the pancreas (Fig. 1 and Table 2). The mean SUV in head, body, and tail was 4.5, 2.4, and 4.1 g/ml, respectively. In 2001 relaparotomy was performed and a near-total pancreatectomy, guided by PET and preserving only the unaffected part of the head of the pancreas, was performed. Histological analysis showed typical findings of focal β-cell hyperplasia (Fig. 2). Thereafter, the patient was entirely asymptomatic and normoglycemic, and follow-up was discontinued in June 2005.

A 63-yr-old man (patient 2) was admitted to our hospital with a history of nausea, fatigue, and hypoglycemia for 2 yr in 2001. The fasting blood glucose test was abnormal (plasma glucose, 2.0 mmol/liter; serum insulin, 24 mU/liter; plasma C-peptide, 1.8 nmol/liter). CT, MRI, and SRS did not reveal a tumorous lesion in the pancreas, whereas ^{18}F-DOPA PET showed a focal lesion in the head of the pancreas (Table 2). The mean SUV in head, body, and tail was 3.0, 2.4, and 2.7 g/ml, respectively. The patient underwent laparotomy for a presumed insulinoma, but no palpable abnormality in the pancreas was found. Under a suspected diagnosis of insulinoma, a subtotal standard resection of the pancreas with splenectomy was performed, leaving the head of the pancreas intact. Histological examination of the resected specimen revealed focal hyperplasia of islet cells, and also the proximal resection margin contained a microscopic focus of nesidioblastosis (Fig. 2), whereas the major part of resected pancreas was considered to be normal. Postoperatively, the patient has remained symptomatic. The most effective medication during these years has been a long-acting calcium channel blocker. Repeated ^{18}F-DOPA PET showed intense

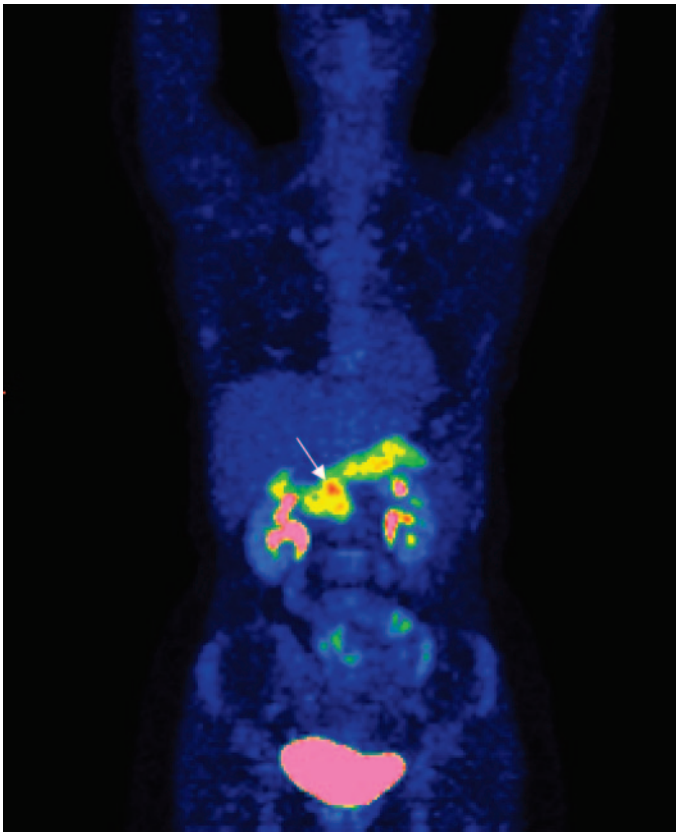

FIG. 1. A 34-yr-old woman (patient 1) with severe symptoms and focal β-cell hyperplasia imaged with ^{18}F-DOPA PET (MIP image). *Arrow* shows the focal lesion in the head of the pancreas.

uptake in the pancreas remnant consistent with residual nesidioblastosis. Both patients with β-cell hyperplasia (no. 1 and 2) had the genomic DNA analyzed for mutations in the *SUR1* and the *Kir6.2* genes, which encode the subunits of the pancreatic ATP-sensitive potassium channel responsible for glucose-induced insulin secretion (1). No mutations were found in either of these genes.

Patients with insulinomas had a varying degree of symptoms and signs (Table 1). A typical case is a previously healthy 53-yr-old man (patient 9) who presented in July 2004 with a 2-yr history of episodes of seizures. Laboratory studies during evaluation revealed a plasma glucose level of 2.2 mmol/liter with a concomitant serum insulin level of 8 mU/liter. Neither contrast CT nor MRI was able to detect a pancreatic tumor. Four months later, ^{18}F-DOPA PET showed enhanced focal uptake in the head of pancreas (Fig. 3). When laparotomy was performed in January 2005, a 1-cm tumor in the head of the pancreas was found, and pancreaticoduodenectomy was performed. The pathological diagnosis was insulinoma. Postoperatively, the patient has remained entirely asymptomatic.

A patient with malignant insulinoma. A 52-yr-old woman (patient 5) had been followed up and treated with octreotide for 3 yr because of a NET with liver metastasis of unknown origin. In 2002, hypoglycemic cramps associated with hyperinsulinism developed. She needed a constant glucose infusion, which was followed by extensive weight gain (up to 1 kg/d). Repeated CT showed only metastasis in the liver but failed to detect the primary tumor. ^{18}F-DOPA PET showed enhanced uptake at the head-body junction of pancreas (Fig. 4). Thus, PET strongly suggested that hypoglycemic episodes were due to an insulinoma in the pancreatic body. In September 2002, a firm tumor smaller than 3 cm was found at laparotomy in agreement with the findings in PET. The body and tail of the pancreas were resected, and final diagnosis was malignant insulinoma with metastases in the liver. After 4 months of remission, the disease progressed. Thereafter she was treated with chemotherapy until late 2003, and she died 2 months after finishing the oncological treatment.

^{18}F-DOPA PET

The pancreas was visible in all patients on ^{18}F-DOPA PET scans. Both patients with focal β-cell hyperplasia (patients 1 and 2) had an area of increased uptake of ^{18}F-DOPA (Fig 1). By visual inspection, it was possible to localize the lesion in six of seven patients with insulinoma using ^{18}F-DOPA PET (Table 2 and Figs. 3 and 4).

The semiquantitative analysis was performed in nine patients, whereas in one patient (no. 7) high tracer uptake in bile made the analysis unreliable. In the remaining nine study patients, the mean and maximum SUV was 4.4 ± 1.0 and 6.7 ± 2.0 g/ml in the affected pancreas and 3.2 ± 1.0 and 5.1 ± 1.6 g/ml, respectively, in other parts of the pancreas. In

TABLE 2. Results of the imaging studies and findings at operation

Patient no.	PET	SUV_{mean} in pancreatic lesion (g/ml)	SUV_{mean} in normal pancreatic tissue (g/ml)[a]	CV (%)	CT	MRI	SRS	IOUS/EUS	Palpation	Size of lesion (cm)
1	+	4.5	3.2	22	−	−	−	−	−	2
2	+	3.0	2.5	15	−	−	ND	ND	−	3
3	+	3.0	2.0	25	+	ND	ND	ND	+	1.3
4	+	4.5	3.0	19	−/+[b]	ND	ND	ND	+	1
5	+	3.9	3.1	21	−	−	ND	ND	+	2
6	+	4.5	2.8	24	+	ND	ND	ND	+	2.7
7	ID	ID	ID	ID	−	+	ND	+	+	2
8	+	5.8	4.3	28	−	−	−	+	+	1.5
9	+	5.0	3.4	38	−	−	ND	ND	+	1
10	+	5.2	4.7	13	−	−	ND	−	+	1

ID, Indeterminate (abundance of radioactivity in bile in common bile duct covering the head of pancreas disturbed the analysis); IOUS, intraoperative ultrasound; ND, not done.

[a] Mean value of SUV_{mean} in normal parts of the pancreas.

[b] Lesion was not detected at the initial CT but could be verified retrospect with knowledge of the PET results.

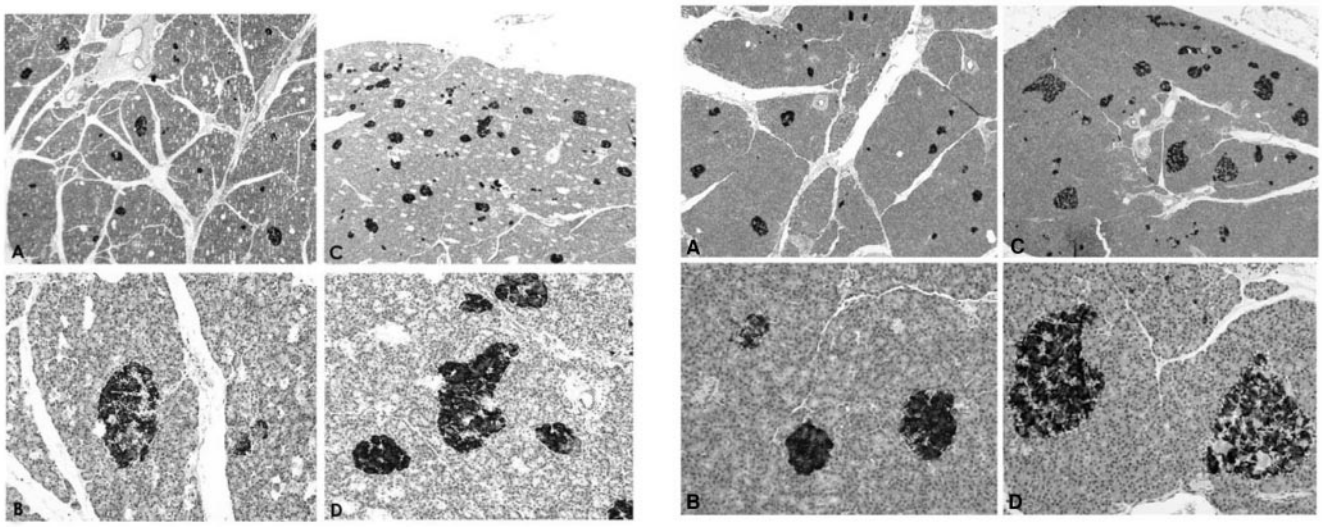

FIG. 2. Patient 1 (*left*) and patient 2 (*right*) with focal β-cell hyperplasia with normal pancreatic tissue areas (A, B) in immunohistochemical staining for insulin and abnormal areas with enlarged islets (C) with nuclear pleomorphism (D). Original magnification, ×200 and ×400.

control patients with nonpancreatic NET, SUV_{mean} of head, body, and tail was 4.4 ± 1.0, 3.9 ± 1.6, and 4.6 ± 1.7 g/ml, and SUV_{max} was 6.8 ± 1.4, 5.6 ± 2.3, and 7.2 ± 2.6 g/ml, respectively. Accumulation of ^{18}F-DOPA seemed to be more homogenous in control patients, but no significant difference was found in maximum or mean SUV values between patients with and without pancreatic tumor lesions. In general, the body of the pancreas showed 18 ± 8% lower tracer uptake

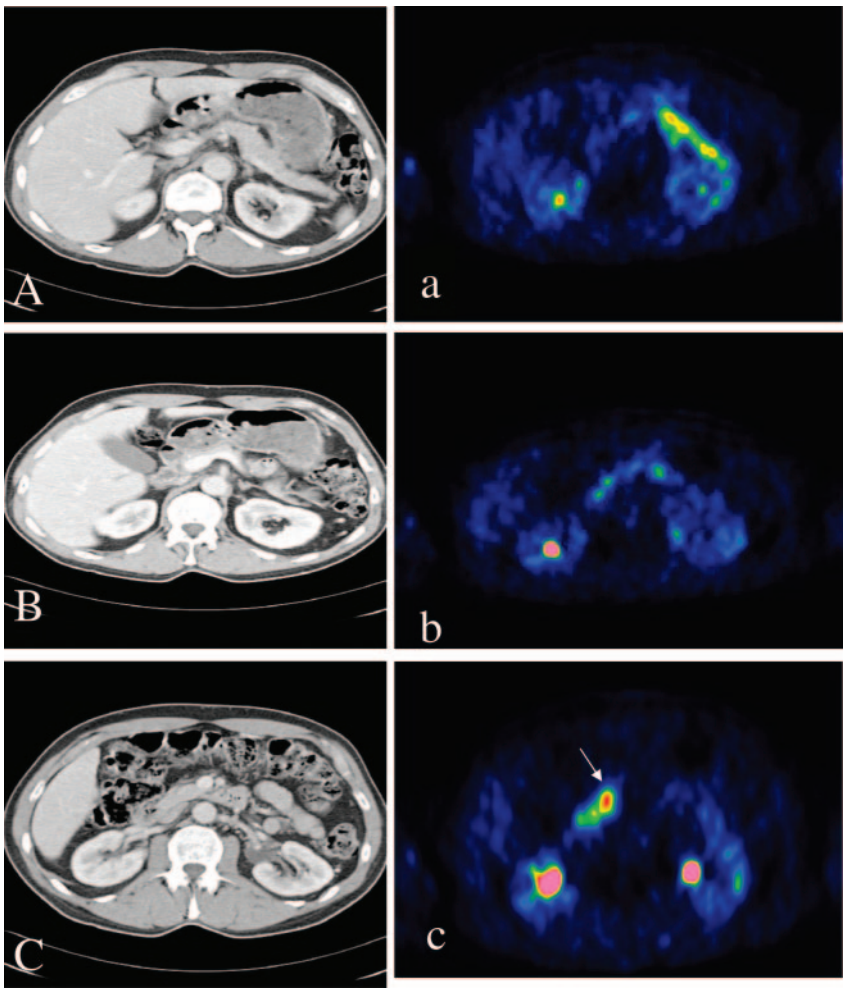

FIG. 3. In PET scans, the focus of insulinoma is shown as an increased accumulation of ^{18}F-DOPA in the head of the pancreas (*arrow*), whereas the CT finding is negative (patient 9). Corresponding transaxial image slices of CT (*left*) and ^{18}F-DOPA PET (*right*) are shown: tail (Aa) of the pancreas (SUV_{max} 5.4); body (Bb) of the pancreas (SUV_{max} 4.2); and head (Cc) of the pancreas (SUV_{max} 8.7).

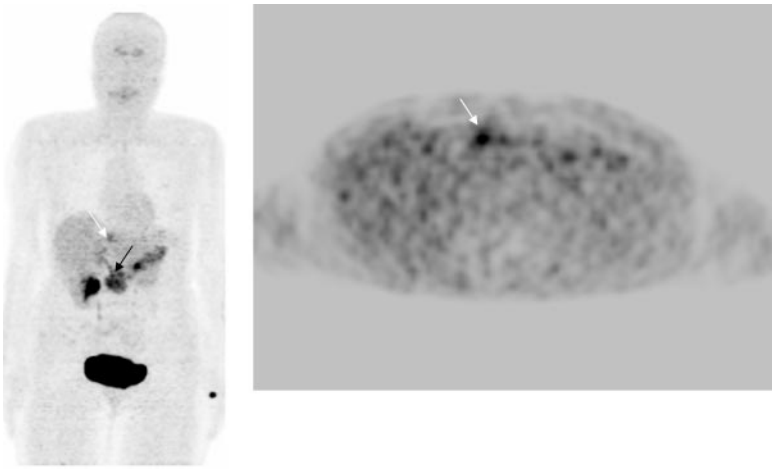

FIG. 4. In a patient with malignant insulinoma with metastasis in the liver (patient 5), the lesion is not found in the pancreas in MRI or CT. ^{18}F-DOPA PET shows primary tumor at the head-body junction of the pancreas (*black arrow*) and liver metastasis (*white arrow*).

compared with the rest of the pancreas in both study and control patients.

^{18}F-DOPA PET vs. CT and MRI

The sensitivity of ^{18}F-DOPA PET was 90% [95% confidence interval (CI), 56–99%] to identify the disease focus in patients with PHH, whereas the sensitivity of CT was 30% (95% CI, 7–65%) and MRI was 40% (95% CI, 12–74%). CT and MRI were negative in both patients with β-cell hyperplasia. By contrast, in four patients with insulinoma, CT (three of eight) or MRI (one of five) also showed the lesion (Table 2). In five of 10 patients, ^{18}F-DOPA PET provided additional information for surgery that was obtained with none of the other imaging procedures. Difference in classification between PET and CT was significant ($P = 0.031$), and between PET and MRI the difference remained nonsignificant ($P = 0.125$). The κ coefficient for agreement was negligible ($\kappa = 0.09$) for PET and CT, and that for PET and MRI ($\kappa = -0.21$) was negative, respectively. The latter was due to being as conservative as possible in statistical analysis and required MRI to be considered as positive whenever it was not actually performed (three cases). Similarly, CT was regarded as positive in patient 4, in whom the lesion was only detected in retrospect with knowledge of PET results.

Management, histology, and outcome

All patients underwent operation. The tumors were bimanually palpable in eight patients, whereas in the case of β-cell hyperplasia (patients 1 and 2), no palpable tumors were found. Insulinomas were enucleated in three patients. A subtotal pancreatic resection was necessary in seven patients, and three of those patients also underwent splenectomy. Only one patient required a pancreaticoduodenectomy (Table 1). The primary tumors were distributed throughout the pancreas and ranged from 1.0–3.0 cm in diameter. In seven of 10 patients, the tumors had typical histological characteristics of insulinoma, such as insulin-producing β-cells with amyloid stroma. One patient (no. 5) had a malignant insulinoma in addition to liver metastases. Two patients had a focal form of β-cell hyperplasia. In those patients, morphological findings included hypertrophic islets showing β-cells with enlarged nuclei, increased numbers of islet cells budding off ducts, and neoformation of islets from ducts (Fig. 2).

Hypoglycemia symptoms disappeared after operation in nine patients. Only one patient (no. 2), who had β-cell hyperplasia of the head of the pancreas, remained symptomatic after operation. One patient (no. 6) had a complication related to the pancreatic enucleation, resulting in severe pancreatitis, leading to death. Patient 5, who had malignant insulinoma with liver metastases, died 15 months postoperatively.

Discussion

This study shows that ^{18}F-DOPA PET is a sensitive novel imaging method to identify the disease focus in patients with PHH caused by either insulinoma or β-cell hyperplasia. Furthermore, current findings indicate that ^{18}F-DOPA PET seems to be more sensitive in localizing the disease focus compared with both CT and MRI. However, a variety of factors may influence the ability of ^{18}F-DOPA PET to localize a tumor. The physiological uptake of L-DOPA in the duodenum and pancreas might cause false-positive results. Furthermore, imaging of the upper abdomen including the pancreas is likely to be influenced by respiratory motion (27).

PET provides the opportunity to design tracers chemically close or identical to physiological substrates, which is of interest in NET research (12). Increased activity of L-DOPA decarboxylase was found to be characteristic of NET (28). According to previous immunohistochemical studies, pancreatic β-cells can also take up amine precursors, like L-DOPA, and convert them into dopamine by L-DOPA decarboxylase (13, 29, 30). The radiolabeled L-DOPA is transported across the β-cell membrane by an amino acid transporter, after which it is decarboxylated into ^{18}F-fluoro-dopamine and stored in vesicles.

At present, the preoperative planning in the treatment of insulinoma or β-cell hyperplasia is significantly restricted by the limited preoperative knowledge of the location of the lesion. On the basis of our results, ^{18}F-DOPA PET was a significantly more sensitive imaging method to identify the disease focus in patients with PHH compared with CT or MRI. We found focal accumulation of ^{18}F-DOPA in the pan-

creas of nine of 10 patients, and the focal lesion was confirmed histologically as an insulinoma or β-cell hyperplasia in all 10 patients. All patients underwent limited pancreatic resection (seven of 10) or enucleation (three of 10). In line with infants, our experience with adult patients indicates that the functional imaging with ^{18}F-DOPA PET might help to optimize surgical treatment of focal β-cell hyperplasia. So far, β-cell hyperplasia is a rare and poorly characterized disease. Recently, there has been rising interest in this disease as a cause of PHH in adults (2, 8–10). Anlauf *et al.* (2) reported a series of 232 adult patients with PHH. Ten of those patients (4.3%) histologically showed the features of β-cell hyperplasia. In a recent study, Service *et al.* (8) reported six cases of β-cell hyperplasia occurring in patients who had undergone gastric bypass surgery as treatment for severe obesity.

Surgical excision of the lesion is the primary mode of treatment, and patients are almost invariably cured for life with complete excision of a solitary benign insulinoma. Accurate localization of these small tumors provides important support for the surgeon, limiting the surgical exploration and therewith the morbidity. However, the precise preoperative localization of these lesions has remained a clinical problem. Earlier, routine blind subtotal distal pancreatectomy was the treatment of choice (31–33). Nowadays, treatment is accomplished by enucleation or partial pancreatic resection. In recent years, however, advanced laparoscopic techniques have been used to resect islet cell tumors in a few patients (34, 35). This novel surgical approach makes preoperative imaging even more important due to lack of bimanual palpation.

The major limitation of the present study was the small number of patients, due to the rarity of the disease. Although the small sample size limits the analysis, our study is unique because it includes a population imaged at one institute. Another limitation is that conventional imaging studies (CT, MRI, SRS, and EUS) were not performed systematically in all patients.

In conclusion, ^{18}F-DOPA PET seems to be superior to CT or MRI in localizing insulinoma or β-cell hyperplasia. Because L-DOPA also accumulates physiologically in the normal pancreas, ^{18}F-DOPA PET is a useful diagnostic tool only for patients with confirmed inappropriate insulin secretion. Future studies are likely to be performed with hybrid PET/CT scanners, which enable correlation of anatomical and functional information within one imaging session. In addition, externally triggered respiratory gating may further improve the diagnostic accuracy of PET images in the pancreas. It is expected that the results obtained in the present study will provide extensive and useful information for future investigation. Therefore, ^{18}F-DOPA PET has the potential to become the functional imaging method of the future, once the results reported here are confirmed in a larger patient population.

Acknowledgments

The authors thank the staff of Turku Cyclotron and the Radiochemistry Laboratory for technical support and advice and the staff of Turku PET Centre for excellent help in imaging the patients. We also thank Professor M. Laakso and Dr. H. Huopio from University Central Hospital of Kuopio for their help in genetic analyses and acknowledge Irina Lisinen and Hans Helenius for consultation on the statistical analyses.

Received July 11, 2006. Accepted January 5, 2007.

Address all correspondence and requests for reprints to: Pirjo Nuutila, M.D., Turku PET Centre, Turku University Hospital, P.O. Box 52, FIN-20521 Turku, Finland. E-mail: pirjo.nuutila@tyks.fi.

This study was supported by a grant from the University Central Hospital of Turku (EVO grant) and the Novo Nordisk Foundation.

Disclosure Summary: All authors have nothing to declare.

References

1. **Service FJ, Natt N, Thompson GB** 1999 Noninsulinoma pancreatogenous hypoglycemia: a novel syndrome of hyperinsulinemic hypoglycemia in adults independent of mutations in Kir6.2 and SUR1 genes. J Clin Endocrinol Metab 84:1582–1589
2. **Anlauf M, Wieben D, Perren A** 2005 Persistent hyperinsulinemic hypoglycemia in 15 adults with diffuse nesidioblastosis: diagnostic criteria, incidence, and characterization of β-cell changes. Am J Surg Pathol 29:524–533
3. **McAuley G, Delaney H, Colville J** 2005 Multimodality preoperative imaging of pancreatic insulinomas. Clin Radiol 60:1039–1050
4. **Grant CS** 2005 Insulinoma. Best Pract Res Clin Gastroenterol 19:783–798
5. **Carlson T, Eckhauser ML, DeBaz B, Khiyami A, Park CH** 1987 Nesidioblastosis in an adult: an illustrative case and collective review. Am J Gastroenterol 82:566–571
6. **Hirshberg B, Cochran C, Skarulis MC** 2005 Malignant insulinoma: spectrum of unusual clinical features. Cancer 104:264–272
7. **Yakovac WC, Baker L, Hummeler K** 1971 β-Cell nesidioblastosis in idiopathic hypoglycemia of infancy. J Pediatr 79:226–231
8. **Service GJ, Thompson GB, Service FJ, Andrews JC, Collazo-Clavell ML, Lloyd RV** 2005 Hyperinsulinemic hypoglycemia with nesidioblastosis after gastric-bypass surgery. N Engl J Med 353:249–254
9. **Tsujino M, Sugiyama T, Nishida K** 2005 Noninsulinoma pancreatogenous hypoglycemia syndrome: a rare case of adult-onset nesidioblastosis. Intern Med 44:843–847
10. **Jabri AL, Bayard C** 2004 Nesidioblastosis associated with hyperinsulinemic hypoglycemia in adults: review of the literature. Eur J Intern Med 15:407–410
11. **Chatzioannou A, Kehagias D, Mourikis D** 2001 Imaging and localization of pancreatic insulinomas. Clin Imaging 25:275–283
12. **Eriksson B, Orlefors H, Oberg K, Sundin A, Bergstrom M, Langstrom B** 2005 Developments in PET for the detection of endocrine tumours. Best Pract Res Clin Endocrinol Metab 19:311–324
13. **Ericson LE, Hakanson R, Lundquist I** 1977 Accumulation of dopamine in mouse pancreatic B-cells following injection of L-DOPA. Localization to secretory granules and inhibition of insulin secretion. Diabetologia 13:117–124
14. **Cegrell L** 1968 The occurrence of biogenic monoamines in the mammalian endocrine pancreas. Acta Physiol Scand Suppl 314:1–60
15. **Ahlstrom H, Eriksson B, Bergstrom M, Bjurling P, Langstrom B, Oberg K** 1995 Pancreatic neuroendocrine tumors: diagnosis with PET. Radiology 195: 333–337
16. **Eriksson B, Bergstrom M, Sundin A** 2002 The role of PET in localization of neuroendocrine and adrenocortical tumors. Ann NY Acad Sci 970:159–169
17. **Anderson CJ, Dehdashti F, Cutler PD** 2001 64Cu-TETA-octreotide as a PET imaging agent for patients with neuroendocrine tumors. J Nucl Med 42:213–221
18. **Hoegerle S, Altehoefer C, Ghanem N** 2001 Whole-body 18F dopa PET for detection of gastrointestinal carcinoid tumors. Radiology 220:373–380
19. **Hoegerle S, Ghanem N, Altehoefer C** 2003 18F-DOPA positron emission tomography for the detection of glomus tumours. Eur J Nucl Med Mol Imaging 30:689–694
20. **Hoegerle S, Nitzsche E, Altehoefer C** 2002 Pheochromocytomas: detection with 18F DOPA whole body PET—initial results. Radiology 222:507–512
21. **Hoegerle S, Altehoefer C, Ghanem N, Brink I, Moser E, Nitzsche E** 2001 18F-DOPA positron emission tomography for tumour detection in patients with medullary thyroid carcinoma and elevated calcitonin levels. Eur J Nucl Med 28:64–71
22. **Becherer A, Szabo M, Karanikas G** 2004 Imaging of advanced neuroendocrine tumors with (18)F-FDOPA PET. J Nucl Med 45:1161–1167
23. **Otonkoski T, Nanto-Salonen K, Seppanen M** 2006 Noninvasive diagnosis of focal hyperinsulinism of infancy with [18F]-DOPA positron emission tomography. Diabetes 55:13–18
24. **Ribeiro MJ, de Lonlay P, Delzescaux T** 2005 Characterization of hyperinsulinism in infancy assessed with PET and 18F-fluoro-L-DOPA. J Nucl Med 46:560–566
25. **Hussain K, Seppanen M, Nanto-Salonen K, Adzick NS, Stanley CA, Thornton P, Minn H** 2006 The diagnosis of ectopic focal hyperinsulinism of infancy with [18F]-DOPA positron emission tomography. J Clin Endocrinol Metab 91:2839–2842
26. **Bergman J, Haaparanta M, Lehikoinen P, Solin O** 1994 Electrophilic synthesis of 6–18Ffuoro-L-dopa starting from aqueous-18Ffluoride. J Labelled Comp Radiopharm 35:476–477
27. **Boucher L, Rodrigue S, Lecomte R, Benard F** 2004 Respiratory gating for

3-dimensional PET of the thorax: feasibility and initial results. J Nucl Med 45:214–219
28. **Gazdar AF, Helman LJ, Israel MA** 1988 Expression of neuroendocrine cell markers L-DOPA decarboxylase, chromogranin A, and dense core granules in human tumors of endocrine and nonendocrine origin. Cancer Res 48:4078–4082
29. **de Lonlay P, Simon-Carre A, Ribeiro MJ** 2006 Congenital hyperinsulinism: pancreatic [18F]fluoro-L-dihydroxyphenylalanine (DOPA) positron emission tomography and immunohistochemistry study of DOPA decarboxylase and insulin secretion. J Clin Endocrinol Metab 91:933–940
30. **Borelli MI, Villar MJ, Orezzoli A, Gagliardino JJ** 1997 Presence of DOPA decarboxylase and its localisation in adult rat pancreatic islet cells. Diabetes Metab 23:161–163
31. **Kaczirek K, Ba-Ssalamah A, Schima W, Niederle B** 2004 The importance of preoperative localisation procedures in organic hyperinsulinism–experience in 67 patients. Wien Klin Wochenschr 116:373–378
32. **Hirshberg B, Libutti SK, Alexander HR** 2002 Blind distal pancreatectomy for occult insulinoma, an inadvisable procedure. J Am Coll Surg 194:761–764
33. **Kuzin NM, Egorov AV, Kondrashin SA, Lotov AN, Kuznetzov NS, Majorova JB** 1998 Preoperative and intraoperative topographic diagnosis of insulinomas. World J Surg 22:593–597
34. **Jaroszewski DE, Schlinkert RT, Thompson GB, Schlinkert DK** 2004 Laparoscopic localization and resection of insulinomas. Arch Surg 139:270–274
35. **Assalia A, Gagner M** 2004 Laparoscopic pancreatic surgery for islet cell tumors of the pancreas. World J Surg 28:1239–1247

JCEM is published monthly by The Endocrine Society (http://www.endo-society.org), the foremost professional society serving the endocrine community.